U.S. ARMY COMBAT CAPABILITIES DEVELOPMENT COMMAND
CHEMICAL BIOLOGICAL CENTER

ABERDEEN PROVING GROUND, MD 21010-5424

DEVCOM CBC-TR-1798

The Role of Turbulence Intensity and Aerosol Stokes Number in Isokinetic Sampling Techniques

Daniel Wise
Daniel Weber

RESEARCH AND TECHNOLOGY DIRECTORATE

January 2023

Disclaimer

The findings in this report are not to be construed as an official Department of the Army position unless so designated by other authorizing documents.

REPORT DOCUMENTATION PAGE

Form Approved
OMB No. 0704-0188

1. REPORT DATE *(DD-MM-YYYY)*	**2. REPORT TYPE**	**3. DATES COVERED** *(From - To)*
XX-01-2023	Final	May 2011–Aug 2011

4. TITLE AND SUBTITLE
The Role of Turbulence Intensity and Aerosol Stokes Number in Isokinetic Sampling Techniques

5a. CONTRACT NUMBER

5b. GRANT NUMBER

5c. PROGRAM ELEMENT NUMBER

6. AUTHOR(S)
Wise, Daniel and *Weber, Daniel (DEVCOM CBC)

5d. PROJECT NUMBER

5e. TASK NUMBER

5f. WORK UNIT NUMBER

7. PERFORMING ORGANIZATION NAME(S) AND ADDRESS(ES)
Director, DEVCOM CBC, ATTN: FCDD-CBR-TS, APG, MD 21010-5424

8. PERFORMING ORGANIZATION REPORT NUMBER
DEVCOM CBC-TR-1798

9. SPONSORING / MONITORING AGENCY NAME(S) AND ADDRESS(ES)
U.S. Army Combat Capabilities Development Command Chemical Biological Center; 8198 Blackhawk Road, Aberdeen Proving Ground, MD

10. SPONSOR/MONITOR'S ACRONYM(S)
DEVCOM CBC

11. SPONSOR/MONITOR'S REPORT NUMBER(S)

12. DISTRIBUTION / AVAILABILITY STATEMENT
Approved for public release: distribution unlimited.

13. SUPPLEMENTARY NOTES
*Daniel Weber is now retired from DEVCOM CBC.
U.S. Army Combat Capabilities Development Command Chemical Biological Center (DEVCOM CBC) was previously known as U.S. Army Edgewood Chemical Biological Center (ECBC).

14. ABSTRACT: (Limit 200 words)
Inlet efficiency measurements were made for a range of thin-walled tube sampling probes by comparing them with a probe of fixed size co-located in a uniform aerosol stream with a 10 mph wind velocity. Free-stream turbulence intensity was varied as part of the experimental matrix. The various levels of turbulence intensity were created using classical types of turbulence grids and a unique new class of "fractal grids", which are reported to have unique turbulence qualities. In our study, isokinetic sampling did not provide the same aerosol concentration across scales of probe diameter. Inlet efficiency increased with the increasing probe Stokes number. This result was more pronounced for low levels of free-stream turbulence.

Unmanned aerial vehicle	Sampling probe	Fractal grid	Drones
Aerosol sampling	Stokes number (*Stk*)	Turbophoresis	Inlet
Computational fluid dynamics (CFD)	Reynolds number (*Re*)	Turbulence	Isokinetic
High wind speed	Wind tunnel		

16. SECURITY CLASSIFICATION OF:			**17. LIMITATION OF ABSTRACT**	**18. NUMBER OF PAGES**	**19a. NAME OF RESPONSIBLE PERSON**
a. REPORT	**b. ABSTRACT**	**c. THIS PAGE**			Renu B. Rastogi
U	U	U	UU	32	**19b. TELEPHONE NUMBER** *(include area code)* (410) 436-7545

Standard Form 298 (Rev. 8-98)
Prescribed by ANSI Std. Z39.18

Blank

PREFACE

The work described in this report was authorized under the U.S. Army Combat Capabilities Development Command Chemical Biological Center (DEVCOM CBC; Aberdeen Proving Ground, MD) Seedling Program The work was started in May 2011 and completed in August 2011.

At the time this work was performed, DEVCOM CBC was known as the U.S. Army Edgewood Chemical Biological Center.

The use of either trade or manufacturers' names in this report does not constitute an official endorsement of any commercial products. This report may not be cited for purposes of advertisement.

This report has been approved for public release.

Acknowledgments

The authors acknowledge the following individuals for their hard work and assistance with the execution of this technical program:

- Christine Franklin (Leidos Corporation; Gunpowder, MD) for administrative support in preparing this document;
- Elias Yoon (formerly of DEVCOM CBC) for contributing to the hot wire anemometer setup;
- Dr. Igor Novosselov (University of Washington; Seattle, WA) for suggesting computational fluid dynamics (CFD) analysis of the observed phenomena, the possible mechanisms by which CFD could occur, and general guidance on experimental combinations; and
- Daniel VanReenen (DEVCOM CBC) for fabricating several test fixtures and the DEVCOM CBC Advanced Design and Manufacturing team for fabricating the novel fractal grid.

Blank

CONTENTS

FIGURES

TABLE

THE ROLE OF TURBULENCE INTENSITY AND AEROSOL STOKES NUMBER IN ISOKINETIC SAMPLING TECHNIQUES

1. INTRODUCTION

Isokinetic sampling is a primary concept in the referencing of aerosols.[1] This sampling technique avoids aerosol collection size and concentration biasing by sampling air iso-axially and matching the velocity of the flow going into the inlet to the approaching wind velocity. This arrangement eliminates streamline curvature as the air moves into the inlet; therefore, it should aspirate aerosol particles with 100% efficiency. For this reason, isokinetic sampling probes are employed in reference sampling systems used in aerosol research, especially in testing of aerosol sampling inlets. A more detailed summary of aerosol samplers and isokinetic probes is presented in Appendix A.

Interesting observations have indicated a point in the scale of aerosol sampling equipment (particularly isokinetic reference probes) at which there is a significant increase in particle loss because of turbulent particle dispersion (i.e., either to turbophoresis or energetic impaction).[2–4] In many situations, especially in windy outdoor sampling environments, the free-stream turbulence intensity can be significantly higher than that inside a smooth sampling probe or tube. One conjecture is that the intensity of the free-stream turbulence causes particle aspiration losses at the leading edge of the probe. Because the trajectories of particles transported by flow are coupled to flow turbulence,[5] small probe diameters are more susceptible to aspiration losses as their physical size is closer to that of the turbulence intensity.[a] Although there is some information relating turbulence to particle aspiration loss,[6] these data do not extend over a wide range of probe diameters, and there is a lack of information that relates turbophoresis or energetic impaction dependence on scale for various levels of turbulence. Furthermore, this dependency is difficult to computationally model because turbulence models for aerosols are unsuitable for handling phenomena such as laminar to turbulent transition and bluff-body aerodynamics that are probably major effects in aerosol aspiration in isokinetic conditions.

An experimental program was designed to investigate the performance of isokinetic probes over a range of physical scales. The objective of the experiments was to determine a critical Stokes number (*Stk*) relating to scale, particle size, and flow velocity at which turbophoresis or energetic impaction affects aerosol aspiration. The relationship of this critical *Stk* to free-stream turbulence intensity was also observed. (A more detailed description of *Stk* and Reynolds number [*Re*] is provided in Appendix B.)

The main goal of the experimental program was to determine whether turbulence intensity is the primary underlying phenomena in the breakdown of isokinetic reference methods and if so, correlate it to a critical inlet Stokes number. The relevance of this study is two-fold. First, it contributes to the accurate referencing of aerosols in experimental studies. It provides the anecdotal advice that reference sampling probes must be selected in context of scale (e.g., small

[a]Turbulence intensity characterizes the magnitude of turbulent fluctuations in air flow. It is defined for a particular location as the ratio root mean square (rms) of velocity fluctuations over time above the average of the velocity over the same period of time.

probes seem to suffer from particle losses). Ignorance of this rule-of thumb guidance can result in unnoticed inaccurate data. Second, validation of the approaches used in numerical simulations (computational fluid dynamics [CFD]) is often lacking. In addition, the models for many physical phenomena are not well developed and are not implemented in commercial CFD codes. In particular, aerosol particle tracking capabilities for purposes of aspiration and transport modeling rely on proper implementation of the effect of turbulence intensity and adequate turbulence models with particle trajectory–turbulence coupling. Performing basic CFD simulations for reference probe geometries and comparing the numerical results with the experimental data obtained from wind tunnel tests can provide necessary confidence in the chosen turbulence model.

2. METHODS

2.1 Overview

Aerosol aspiration experiments using different scale isokinetic sampling probes were performed in an aerosol wind tunnel where free-stream turbulence intensity, *Re*, and *Stk* could be controlled and varied. The turbulence-induced losses were assessed by aspiration efficiency characterization (using a co-located unity probe) as the scale of the test probe was reduced. The experiment was repeated with different levels of turbulence intensity by tailoring of the free stream with turbulence grids. Overall inlet efficiency is a product of aspiration and transport of the particles and is described in more detail in Appendix A. Inlet efficiency is determined by aerosol concentration collected by the probes, including their internal losses, so that differences in the inlet efficiency are attributed only to aspiration. The aspiration efficiency of the test probe should be near unity until the interaction of turbulence intensity with probe scale becomes significant, at which point the aspiration efficiency should drop noticeably. This drop-off would correspond to a particular probe *Re* (the ratio of inertial to viscous forces referenced to the probe diameter) and *Stk* (the ratio of particle response time to fluid time scale or, more generally, the ratio of fluid pressure forces to the viscous forces). The point at which this drop-off occurs is considered the critical *Re* and *Stk* for that turbulence intensity level.

2.2 Experimental Facility

The experiments were performed in an aerosol wind tunnel with a 20 × 20 in. test section. The test aerosol was generated using a vibrating orifice aerosol generator (VOAG; TSI Inc., Shoreview, MN) with a fluorescently tagged oleic acid solution. The wind tunnel was operated at a 10 mph test section velocity for all trials. The VOAG produced 5 μm monodispersed particles, which were introduced to the wind tunnel. Within the wind tunnel, an array of mixing fans mixed those particles with incoming filtered high-efficiency particulate air (HEPA) to produce a uniform aerosol challenge. The seeded airflow then passed through a turbulence/fluctuation dampening screen. The aerosol then passed through a contraction to achieve the desired test velocity in the test section. Free-stream turbulence is then created at the desired intensity by a grid in the fetch upstream of the test section. The subsonic wind tunnel is shown in Figure 1.

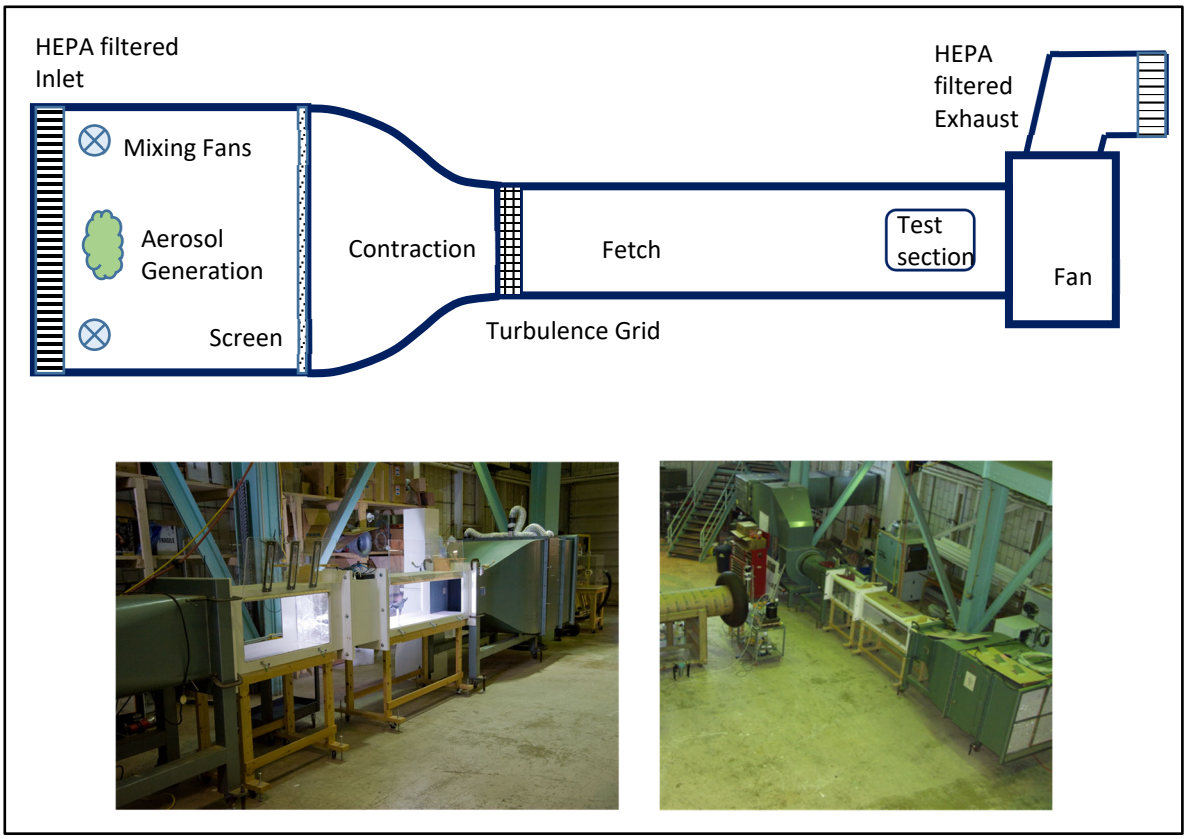

Figure 1. Wind tunnel test facility.

2.3 Test Probes

The experiment was conducted using isokinetic probes of various diameters. The test probes, which were designed in accordance with guidance for thin-walled tube sampling, were attached to a 47 mm glass fiber filter holder via a diverging cone.[7] Thin-walled tubes have been studied extensively, and a deep literature base for reference and comparison exists. The probes used in this study ranged from 0.125 to 1.20 in. in diameter and are shown in Figure 2.

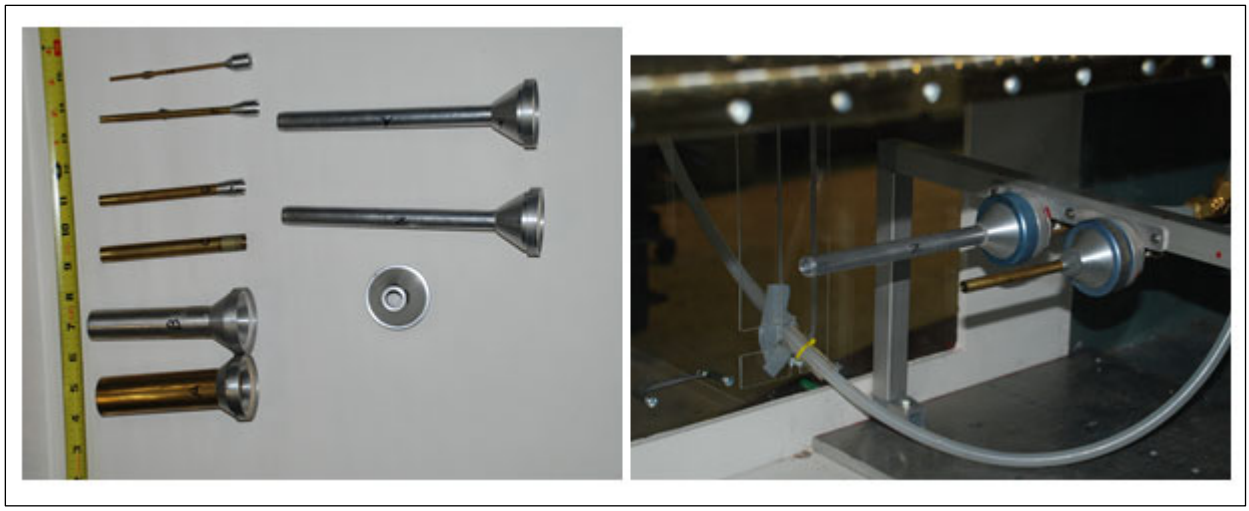

Figure 2. Test probes and test section installation.

2.4 Turbulence Manipulation for Test

This test required different levels of turbulence, which were created by placing a turbulence-generating grid in the wind tunnel upstream of the test probes. Two types of grids were used during the experiments: classical square lattice grids (Figure 3) and a novel fractal grid (Figure 4; briefly discussed in Section 3).

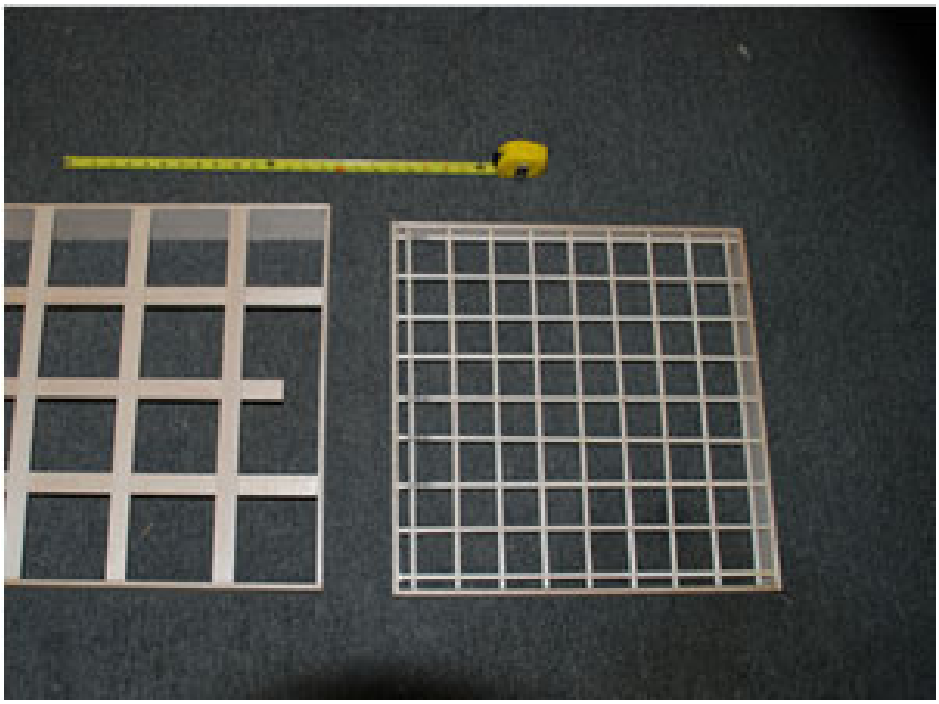

Figure 3. Lattice grids.

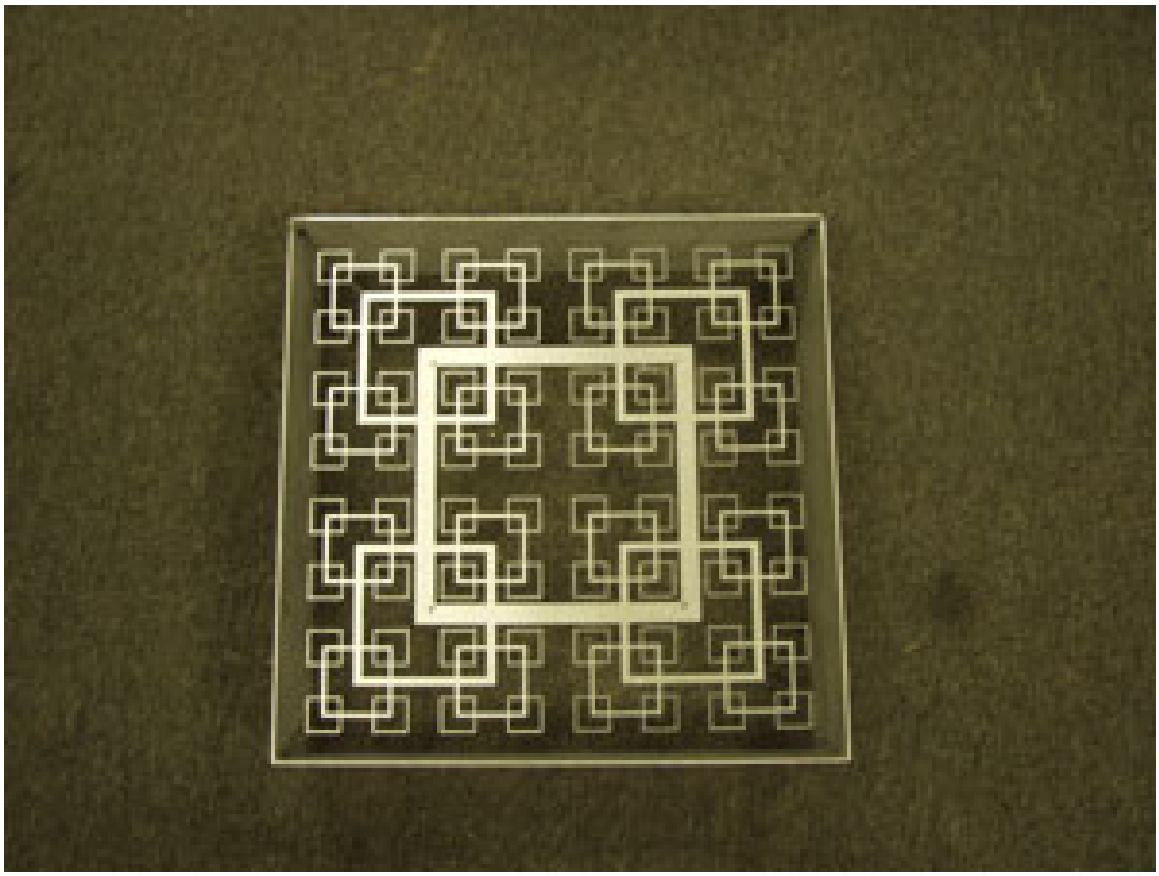

Figure 4. Fractal grid.

2.5. Turbulence Measurements

The centerline test section turbulence level measurements were made in the wind tunnel as different turbulence-generating grids were placed at various upstream locations, relative to the test section, that influenced the magnitude of turbulent energy reaching the test section. A TSI IFA300 thermal anemometry system with ThermoPro (Atlanta, GA) software (version 4.6) was used to make the needed turbulence measurements. A single component TSI model 1262A miniature hotwire probe with a 3.8 μm wire diameter, was used. The probe was calibrated for a 0.11–6.5 m/s velocity range. To properly capture the turbulent influence on the flow field, the velocity must be sampled at a rate sufficient to capture high frequency fluctuations and for a duration sufficient to acquire the low frequency components. The following settings were used: 50 k sample/s sampling rate, low-pass filter with 10 kHz corner frequency, and 20.5 s sampling time. A statistical analysis was performed on these samples to determine the average velocity and turbulence intensity. Turbulence intensity is defined as the rms value of the velocity (turbulence) divided by the average velocity.

3. RESULTS AND DISCUSSION

3.1 Turbulence Manipulation

A key issue in the experimental method was the ability to create turbulence levels of three distinct magnitudes. We have significant experience in dampening existing turbulence for aerodynamic studies and creating turbulence for mixing of test aerosols. However, creation of selectable turbulence levels was unprecedented in our laboratory. Research methods to select turbulence led us beyond classical turbulence grids to a new class of grids referred to as fractal grids. These grids consist of a multi-scale array of planar shapes based on a single pattern that is repeated in increasing number of copies as the scale decreases.[8] The great lure of this class of grid is that the structure of the turbulence is reported to not follow a typical Kolmogorov decay pattern[b] but should produce high levels of turbulence with relatively low pressure drops. This would facilitate the creation of various well characterized turbulence levels at specific down-wind distances. This is an extremely attractive attribute for our experiment. (Moreover, this class of grids creates unique initial conditions for turbulence, which opens new areas of basic research applicable to robust modeling of turbulence.) A fractal grid was fabricated and evaluated (Figure 5), but we were unable to reproduce published turbulence structures. Therefore, the fractal grid was not a solution for all our turbulence test conditions. The fractal grid was used to produce the low- and mid-range turbulence intensity levels; however, a classical, high pressure drop, rectangular grid array was necessary to produce the highest levels of turbulence.

Turbulence measurements were taken under the following conditions:

- the free-stream velocity was set at approximately 10 mph;
- a single turbulence grid was placed in the settling chamber just upstream of the contraction;
- a centerline test section velocity and turbulence measurement was made with the screen installed and fans operating; and
- finally, measurements were taken with the classical grids and the novel fractal grid positioned at several distances from the measuring hotwire in the test section.

The results are shown in Figure 6.

[b]The following description is the author's abbreviated and simple interpretation of Richardson–Kolmogorov Decay relevant to our desire to create a more persistent turbulent structure. Richardson describes turbulent energy transfer from large swirls (eddies) breaking into small swirls. Kolmogorov asserts that the normalized turbulent kinetic energy dissipates at a rate independent of *Re* during this process. For example, this means that given constant viscosity, the difference in average velocity between points in the flow are only dependent on the distance between them and the energy dissipation rate per unit mass. This turbulent redistribution of energy across the range of swirl sizes dissipates according to a universal –5/3 power law.[9,10] It has been reported that turbulent structures produced by fractal grids do not follow this –5/3 power law and exhibit a slower decay.

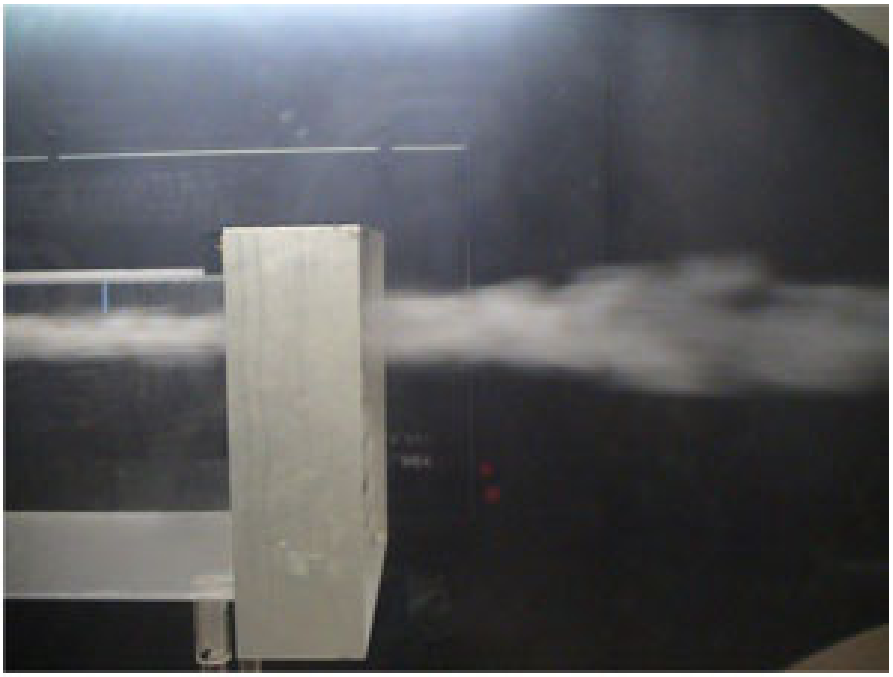

Figure 5. Smoke visualization of fractal grid turbulence.

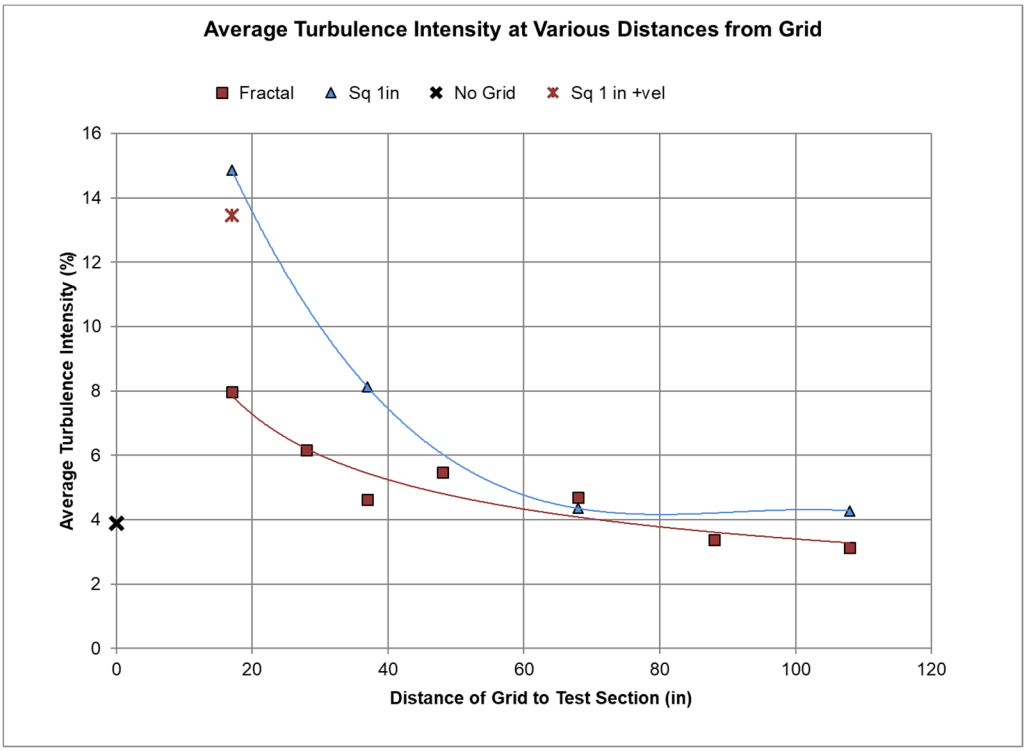

Figure 6. Turbulence intensity as a function of grid distance from test section.

3.2 Aerosol Uniformity

The uniformity of the aerosol challenge was assessed using two identical 0.5 in. probes located at the test and reference probe positions. The overall inlet efficiency determined by comparing these two probes (their concentration ratio) should be unity in a uniform aerosol profile, and the spread of the data over several trials indicates the lowest level of inherent experimental uncertainty. The concentration ratio was 1.06 with a standard deviation of 0.13, which confirmed the test probe arrangement for our study.

3.3 Inlet Efficiency (η_i) over a Range of Probe Diameters and Turbulence Levels

Inlet efficiency (η_i) for different sized isokinetic probes as turbulence intensity varies is shown plotted as a function of either *Re* or the square root of *Stk* ($\sqrt{Stk}$) in Figures 7 and 8, respectively. In expressing similarity of flow and particle inertia conditions, both the *Re* and *Stk* are considered. Both are further explained in Appendix B. Because *Stk* includes both probe diameter and particle size, it is perhaps the best representation to compare to other experimental studies. The error bars are omitted in the $\sqrt{Stk}$ plot for clarity of presentation but retained in the *Re* plot so the degree of uncertainty is visible. The representation of these data as a function of *Re* or $\sqrt{Stk}$ facilitates relating the data to other sampling situations where probe diameter, flow rates, and wind speeds may be different from those tested in this experiment. However, the Table directly indicates the size of our test probes in relation to *Re* and $\sqrt{Stk}$ numbers, as this is of direct practical use to most aerosol sampling test setups.

Table. Probe Diameters and Corresponding *Re* and $\sqrt{Stk}$ Numbers

Probe Diameter (in.)	***Re***	$\sqrt{Stk}$
0.125	937	0.319
0.215	1611	0.245
0.345	2585	0.197
0.500	3747	0.164
0.930	6970	0.124
1.200	8993	0.093

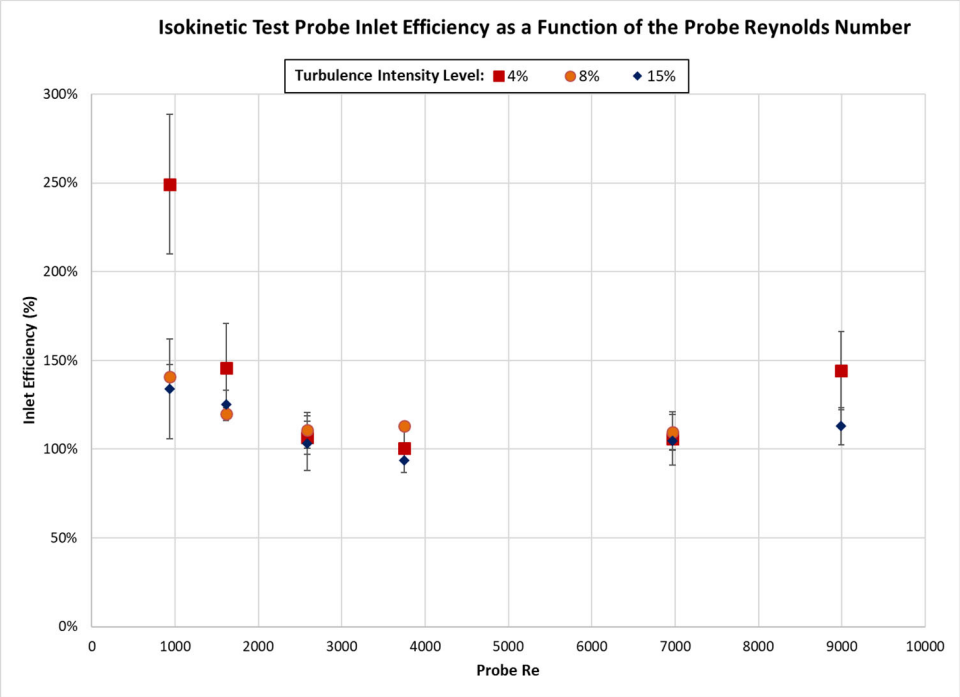

Figure 7. Inlet efficiency as a function of the probe *Re* number.

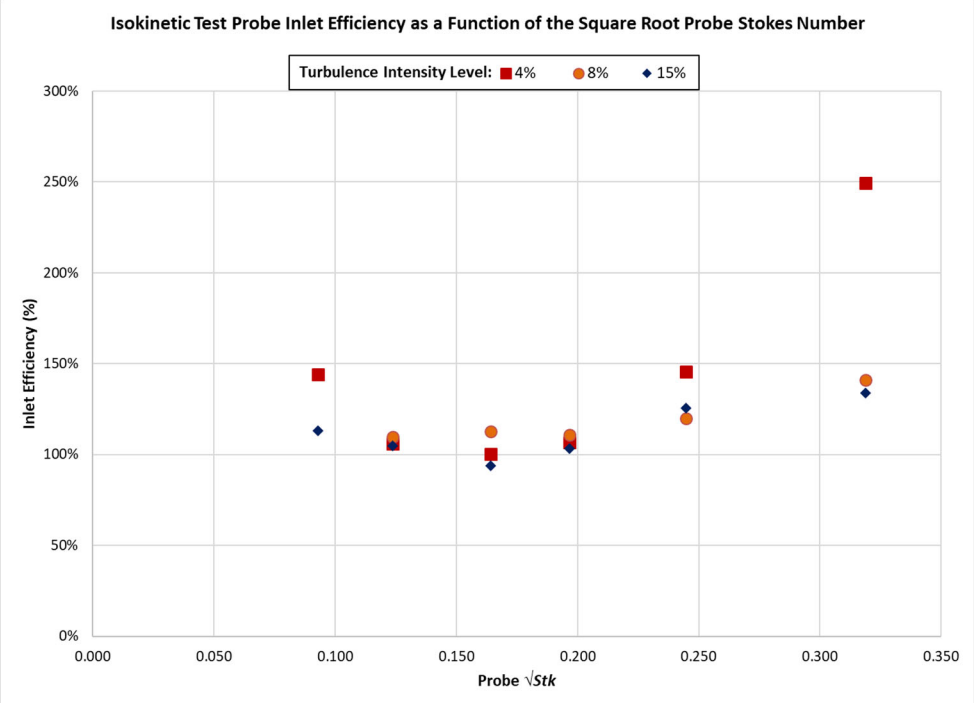

Figure 8. Inlet efficiency as a function of the probe $\sqrt{Stk}$ number.

The mechanism of the aspiration and transport of aerosol through the sampling probe can be better understood if the percent of the aspirated aerosol that is subsequently deposited on the internal surface of the probes is identified. These data were obtained by recovering several rinses of the internal probe surface and are plotted as a function of $\sqrt{Stk}$ and turbulence intensity. The data were supplemented by concurrent but separate data from a setup at much higher wind velocities, which enable the extension of the data range to higher $\sqrt{Stks}$ that were not possible in the small wind tunnel. The rinse data show no strong correlation of internal probe deposition to turbulence intensity except at extreme *Stk* (Figure 9). It is interesting and validating to note that the supplemental data from the independent wind tunnel test match the rinse data from the primary test setup. The extended data show that as the *Stk* increases, there is a point at which the amount of aerosol deposited on the inside of the probe increases rapidly. This has been noted in previous testing of unmanned aerial vehicle mounted samplers at high wind speeds and is of practical rule-of-thumb guidance to testing under those conditions.

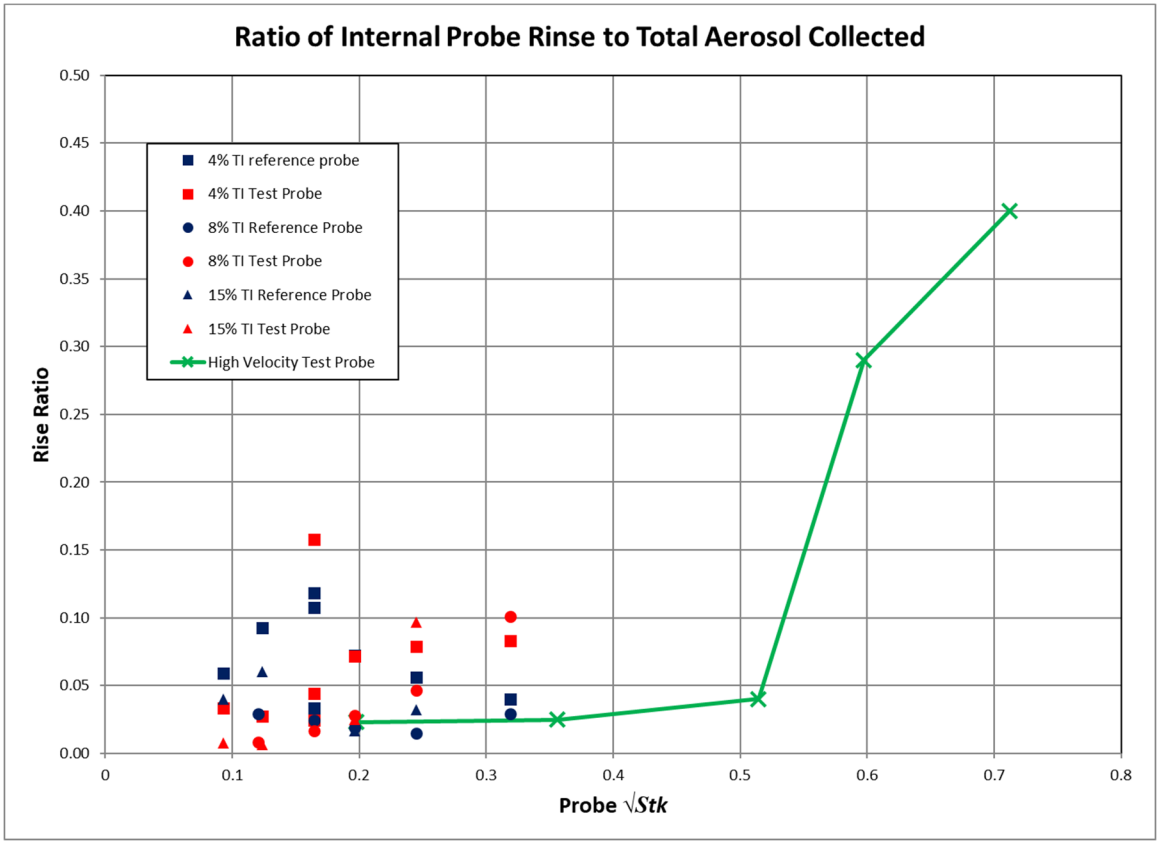

Figure 9. Ratio of internal tube aerosol deposition to total aerosol collected.

The inlet efficiencies for the range of probe sizes and turbulence intensities shown in Figures 7 and 8 indicate an increase in inlet efficiency with increasing *Stk* (i.e., decreasing probe size and *Re*). This result is surprising as previous studies on thin-walled probes showed no effect of turbulence on aspiration efficiency.[6] Therefore, there is no explanation at this time for inlet efficiency greater than unity in our experiment.

When unexplained results occur, the experimental uncertainties should be explored to determine whether the data are truly a physical effect and not just an artifact of the experiment. Admittedly, the measurement of true particle concentration over our wide range of test probes (therefore air flow rates) is extremely difficult. This is reflected to some extent by the magnitude of the error bars for each data point. However, the trend lies outside the trial-to-trial variability. Likely sources of error are the ability to recover deposition from the interior surface of the probes, non-linearity of the fluorometric analysis, and errors in probe sampling air flow rate. Figure 9 rinse data showed that internal probe deposition was not a large percentage of the total signal, (except for the highest *Stk* trials, which were not included in the concentration ratio data) and that the rinses did effectively recover the interior deposition. Any scenario with inadequate probe rinsing would have produced an effect opposite of that observed. The fluorimeter linearity was verified, and the air flow rates, which were held constant from trial-to-trial by critical orifices, were checked with several different calibrated mass flow meters. None of these likely sources of experimental error can account for the unexpected data trend. Therefore, the data suggest that there is a critical *Re*, or more comprehensively, a critical *Stk*, which demarks the breakdown of isokinetic sampling principles. However, the observed effect is opposite our expectations. A very practical objective of performing this experiment was to give some guidance as to the size range of the probes that can be expected to be used as reliable isokinetic reference probes. The data presented in Figures 8 and 9 show that probes with diameters ≤0.25 in. did not work well as isokinetic reference probes.

The scale aspect of this phenomenon has been observed and mentioned previously.[2–4] It is often attributed to experimental uncertainty or inability to account for internally deposited aerosols. One of our objectives was to obtain experimental data on this phenomenon of non-unity concentration ratios for small scale probes and eliminate these two possibilities. The observed non-unity concentration ratio seems to be beyond accountable experimental uncertainty; therefore, other theories to support these results might be pursued. The theory that the probe's *aspiration efficiency* is affected by a large difference in turbulence intensity between free-stream levels and those inside the probe can be strengthened by assessing the turbulence levels inside the probes. This is very difficult to do on such small probes, but it is possible. Furthermore, CFD modeling may be able to shed light on the magnitude of the turbulence difference if several different turbulence models were used to see if any predict these results. If so, then the difference in the models would be a clue to the mechanism for the non-unity concentration ratio. Also, if a turbulence mismatch effect is identified, then our experiment could serve as a verification dataset in the choice of turbulence models used in CFD aerosol sampling design applications.

4. CONCLUSIONS

Inlet efficiency measurements were made for a range of thin-walled tube sampling probes by comparing them to a probe of fixed size co-located in a uniform aerosol stream with a wind velocity of 10 mph. Free-stream turbulence intensity was varied as part of the experimental matrix. The various levels of turbulence intensity were created using classical types of turbulence grids and a unique new class of fractal grids, which are reported to have unique turbulence qualities.

The data indicate that isokinetic sampling does not provide the same aerosol concentration across scales of probe diameter. Probe diameters between 0.345 and 0.93 in. performed well as isokinetic references, but probe diameters outside that range did not reliably yield 100% inlet efficiency. This results in limiting the comfort level of isokinetic probe conditions to a critical *Stk* below $\sqrt{Stk} = 0.2$. Furthermore, the inlet efficiency increased with increasing probe *Stk* for low levels of free-stream turbulence but not so much for high levels of turbulence. We do not understand how this concentration ratio can increase beyond unity, and the experimental uncertainties alone do not seem to account for it. It is suggested that this is possibly a real effect of turbulence intensity mismatch. Follow-on work with turbulence measurements inside the probes and CFD modeling of the sampling situation with different turbulence models can provide a better understanding of these experimental results and possibly support the conjecture that they are caused by large differences in turbulence intensity between the external and internal flows.

5. RECOMMENDATIONS

In theory, a properly designed isokinetic reference probe should provide unbiased, 100% inlet efficiency across all particle size ranges and sampling conditions. Our experiment was carefully conducted to examine the anecdotal guidance that probe size affects this assumption in real-life test situations. Our results reinforce these observations. Therefore, it seems that isokinetic reference probe diameters smaller than 0.345 in. (or $\sqrt{Stk}$ above 0.2) should be used with caution and verified in the test setup by comparison to another isokinetic probe that is in the conventional size range of 0.345 to 1.0 in. In general, it is prudent to verify any probe used as an isokinetic reference against another co-located isokinetic probe to assure both are in agreement.

LITERATURE CITED

1. Hinds, William. *Aerosol Technology*, 2nd ed.; John Wiley & Sons: New York, NY, 1999.

2. Chen, Fu-Lin; Ranade, M.B.; Woods, M.; *Project Summary: The PM-10 Samper Evaluation Program: January 1985 to July 1986;* EPA/600/S4-87/004; U.S. Environmental Protection Agency: Washington, DC, 1987.

3. Kesavan, J.; Sutton, T.; Wise, D. *Edgewood Chemical Biological Center's Evaluation of Generation-3 Vendor Aerosol Collection Subsystems*: *Test Report for Department of Homeland Security's Office of Health Affairs*; U.S. Army Edgewood Chemical Biological Center: Aberdeen Proving Ground, MD, 2010.

4. Novosselov, I.; Ariessohn, P. DFU Inlet Test Report. In *Edgewood Chemical Biological Center In-House Laboratory Independent Research Program Annual Report FY11;* U.S. Army Edgewood Chemical Biological Center: Aberdeen Proving Ground, MD, 2011; UNCLASSIFIED Report (ADA562153). https://www.google.com/search?q=%E2%80%9CIn-House+Laboratory+Independent+Research+Program+Annual+Report+FY11#cobssid=s (accessed 31 July 2011).

5. Novosselov, I. University of Washington, Seattle, WA. *Numerical and Experimental Study of Particle Behavior in Isokinetic Probes*; draft proposal based on conversations at 2010 AAAR conference in San Diego, CA with Daniel Wise, U.S. Army Combat Capabilities Development Command Chemical Biological Center, Aberdeen Proving Ground, MD, 2010.

6. Vincent, J. *Aerosol Sampling: Science and Practice*; Wiley: London, UK, 1989.

7. Durham, M.; Lundgren, D. Evaluation of Aerosol Aspiration Efficiency as a Function of Stokes Number, Velocity Ratio and Nozzle Angle. *J. Aerosol Sci.* **1980**, *11*, 179–188.

8. Mazellier, N.; Vassilicos, J. 2010 Turbulence without Richardson-Kolmogorov cascade. *Phys. Fluids* **2010,** *22*, 075101.

9. McDonough, J.M. Introductory Lectures on Turbulence: Physics, Mathematics and Modeling. *Mechanical Engineering Textbook Gallery*, 2, 2007. https://uknowledge.uky.edu/me_textbooks/2 (accessed 31 July 2011).

10. Ortiz-Suslow, D.G.; Wang, Q. An Evaluation of Kolmogorov's −5/3 Power Law Observed Within the Turbulent Airflow Above the Ocean. *Geophys. Res. Lett.* **2019,** *46,* 14,901–14,911. DOI: 10.1029/2019GL085083

Blank

ACRONYMS AND ABBREVIATIONS

CFD	computational fluid dynamics
DEVCOM CBC	U.S. Army Combat Capabilities Development Command Chemical Biological Center
HEPA	high-efficiency particulate air
η_m	inlet efficiency
Re	Reynolds number
rms	root mean square
Stk	Stokes number
VOAG	vibrating orifice aerosol generator

Blank

APPENDIX A
AEROSOL SAMPLING AND SAMPLING EFFICIENCY

A.1 AEROSOL SAMPLERS

Aerosols are defined as small particles that are suspended in air. The study of these particles has significance in many areas such as environmental and health studies, homeland security, and military defense. The aerosol sampler is a critical component for these studies; its role is to extract the aerosol particles from the environment so they can be analyzed.

These aerosol particles have a mass and velocity vector as they are sampled, and therefore have momentum and inertial characteristics.*

In a typical aerosol sampler, the aerosol in the ambient air is first aspirated into the system through the inlet. It is then transported to the rest of the sampler, sometimes through a system of transmission tubes or ducts. Eventually, it is delivered to a collector device, which puts the aerosol particle into a medium for analysis. Because of their inertial characteristics, aerosols resist change in velocity vector as they pass through the sampling train of a sampler. This inertia affects the sampling of an aerosol. For example, it can cause loss of particles to surfaces and hence, a reduction in aerosol concentration, or it can be used to enrich particle concentration in aerosol concentrators.

A.2 CONCEPT OF AEROSOL SAMPLING EFFICIENCY

One of the basic performance parameters for an aerosol sampler is sampling efficiency. In general, sampling efficiency is a measure of the percentage of ambient particles that the sampling system can add to a sample for analysis. It is a combination of aspiration, transport, collection, retention, and recovery efficiencies. Sometimes, confusion arises when the term collection efficiency is used to mean the same thing as sampling efficiency. In this report, the lexicon will be to use the term collection efficiency to mean the measure of particles trapped or collected by the system without regard to its ability to recover those particles in a useful sample for analysis. The term sampling efficiency (η) includes the ability to place those particles in a sample (e.g., particles that are lost to internal surfaces of a system can be thought of as collected but not sampled).

Overall sampling efficiency (η_o) is the ratio of aerosol sampled to the aerosol in the air. It is usually calculated as the ratio of the concentration of particles collected (or particles

*The terms momentum and inertia are oftentimes used interchangeably, even in technical reports. Inertia is regarded as a characteristic or quality of an object that resists a change of velocity or position. It is not a property as it does not have a value. The property that affects inertia is inertial mass. Momentum is a quantification of the concept of inertia, and it is defined as the cross product of a body's mass and velocity vector ($\mathrm{p} = \mathrm{m} \times \vec{\mathbf{v}}$). Objects with a velocity have momentum, which is the measure of that object's resistance to a change in that velocity (i.e., an acceleration). Because aerosol particles have mass and velocity, momentum affects their behavior, but inertia may be used as a qualitative descriptor for that behavior.

collected per volume of air sampled, (C_{col}) to the concentration of particles in the ambient air (C_{amb}).

$$\eta_0 = \frac{C_{col}}{C_{amb}} \quad (1)$$

In addition, each element (k) of the sampler (e.g., the inlet, transport tubing, collector device, etc.) has an associated efficiency (η_k). Because the flow (Q) through such elements is sometimes split for purposes of concentrating the aerosol, the efficiency equation is generalized.

$$\eta_k = \frac{C_{col} \cdot Q_{out}}{C_{in} \cdot Q_{in}} \quad (2)$$

The overall sampling efficiency is the product of these component efficiencies.

$$\eta_0 = \prod \eta_k \quad (3)$$

The sampling efficiency of any particular component (k) is a function of particle momentum (p), which depends on particle mass (m) and the velocity ($\vec{\mathbf{v}}$) at which it is moving ($p = m \times \vec{v}$). The inertial resistance to a change in the velocity vector is related to the particle mass. The mass of a particle is often represented as a function of a particle's aerodynamic size.† Therefore, sampling efficiency is usually represented as a function of particle size. The larger particles will be lost more readily to mechanisms such as surface impaction as flow curves through the sampling train. Moreover, smaller particles will not be as readily concentrated, or captured in collector devices that rely on inertial methods. Particle size distribution of aerosols is commonly measured by mass median aerodynamic diameter. Aerosol particles in the 1–10 μm range are of greatest interest to collectors used in chemical and biological (CB) defense systems, as this is the size where the human respiratory tract is most susceptible to the inhalation and retention of the particles.

In addition to individual sampling train‡ component efficiencies, the overall sampling efficiency is affected by *retention* and *recovery efficiencies*.

Retention efficiency (η_r) is a concept related to sampling efficiency, which describes the ability of the system to retain collected aerosol particles over the duration that the system is collecting. Particles that are collected by the system may be subsequently lost in a re-aerosolization process. Retention efficiency may be time dependent and can be expressed as a rate of particles retained over a given sampling period.

† Aerodynamic size is the diameter of a unit-density sphere that exhibits the same aerodynamic behavior as the actual particle.

‡ The term "sampling train" is used to describe the compilation of individual sampling components through which the aerosol passes in the particle collection process. Typically, this includes an ambient air sampling inlet, internal particle size fractionators, aerosol concentrators, the transport tubing that connects the components, and the aerosol collector itself. These components are usually arranged in series.

Recovery or elution efficiency (η_e) relates to the ability of a system to remove the collected and retained particles from the collection media or surface and place it into a liquid sample.

Overall sampling efficiency determines the sensitivity of the overall detection capability of the system. The individual component efficiencies (sampling, retention, and recovery/elution) indicate where design problems exist or where sampling train improvements are most beneficial.

A.3 CONCEPT OF INLET EFFICIENCY

An air sampler aspirates the aerosol sample to a collector or sensing device through an air inlet. The performance of an inlet can be characterized by its inlet efficiency (η_i), which is the ratio of the aerosol particle concentration that is delivered through the inlet to the true ambient aerosol concentration. The inlet efficiency is unique with regard to component efficiencies because, in addition to particle size, it is also a function of wind speed.

The inlet efficiency (η_i) is a function of the particle's momentum, which depends on its aerodynamic size (mass) and the velocity at which it moves. An ambient air sampler is often placed in an outdoor environment where the ambient wind is usually significant.[§] Furthermore, a sampler may be placed on a moving platform such as naval ships, ground vehicles, aircraft, or as in the case of this report, unmanned aerial systems (UAS) or "drones". In these situations, the wind speeds can be very high. So, the inlet efficiency will be a function of the particle aerodynamic diameter and the approaching wind speed, $\eta_i(d,v)$.

Furthermore, inlet efficiency is the product of *aspiration efficiency* (η_a) and *transmission efficiency* (η_t).

$$\eta_i = \eta_a \cdot \eta_t \tag{4}$$

Aspiration efficiency refers to the ability of the inlet to capture a particle from the surrounding air flow, and transmission efficiency refers to the ability to take an aspirated particle and carry it to the rest of the air sampling train. A particle's momentum could have opposite influence on the inlet's aspiration and transmission efficiencies. As the air flow moves around the inlet, streamline curvature occurs. Particles with lower momentum (e.g., smaller particles) follow the streamlines, whereas particles with greater momentum cross streamlines and travel into the inlet. Once inside the inlet, the particle speed slows to that of the inlet flow velocity, and the particles with greater mass are more likely to be lost to impaction and deposition than those with less inertia. These inertial effects bias the proportion of the aerosol particles that are transmitted to the rest of the sampler. As this is inertial biasing, it usually affects large particle size fraction more than small particle fraction. For example, in an omnidirectional inlet, large particles will probably not be aspirated efficiently. Conversely, the larger particle size fraction concentration can be enriched by directional probe inlets operating in a sub-isokinetic condition.

[§]Test conditions for evaluating aerosol sampling inlets in wind tunnels per USEPA 40 CFR, Part 53 are 2, 8, and 24 km/h. The average ambient wind speed for U.S. cities is between 10 and 19 km/h depending on location and season.

A.4 CONCEPT OF ISOKINETIC SAMPLING AS REFERENCE

Isokinetic sampling techniques avoid inlet biasing of aerosol collection. Isokinetic sampling involves sampling air iso-axially, that is, the flow into the inlet is aligned with the ambient wind direction (a probe pointed into the wind), and the velocity of the air going into the inlet is matched to the wind velocity. In isokinetic sampling, there is no streamline curvature as the air moves into the inlet. An isokinetic probe inlet would therefore have 100% aspiration efficiency.[**] For this reason, isokinetic sampling probes are employed in reference sampling systems used in aerosol wind tunnel tests.

[**]If wind velocity is lower than probe inlet velocity, the probe will be in an "over-sampling" condition and will be biased toward sampling small aerodynamic diameter particles relative to the large aerodynamic diameter particle fraction. Small particles will be able to follow streamlines as they are drawn into the probe inlet, but larger particles will not and therefore, they will be under-represented in the particle fraction. On the other hand, if the wind velocity is higher than the probe inlet velocity, it will be in an "under-sampling" condition and biased toward sampling large particles relative to the small particle fraction. Because the large particles will not be able to follow streamlines around the apparent blunt object that the probe presents to the airflow, they are in essence rammed into the probe, causing enrichment of the large particle fraction. In either case, the small particles are sampled fairly accurately as they easily follow streamlines; however, the large particles can be over- or under-represented because they cross streamlines according to the radius of curvature.

APPENDIX B
BACKGROUND ON REYNOLDS AND STOKES NUMBERS

Aerosol particles in an air flow experience curvilinear motion as the flow streamlines curve around objects (such as a sampling probe) in the flow. When studying aerosol particles in curvilinear motion, there are two dimensionless similarity quantities that are very useful. These are the Reynolds (*Re*) and Stokes numbers (*Stk*).

To ensure similarity of particle motion around an object such as a sampling probe, the flow *Re* and the particle's *Stk* should be equal. Equal *Re* ensures that the flow patterns are similar, and equal *Stk* assures that the particle motion in that flow field is similar.

- *Re*: The *Re* is a dimensionless ratio of the inertial to the viscous forces in a fluid (air) flow:

$$Re = \frac{\mathrm{V} d_c}{\nu}$$

where *V* is the fluid velocity, d_c is typically the characteristic dimension probe diameter in our study, and *v* is the fluid kinematic viscosity. Note that $\upsilon = \frac{\mu}{\rho_g}$, where μ is absolute or dynamic viscosity and ρ_g is the density of the fluid (air).

Re is useful in determining the laminar or turbulent nature of air flow and can be used to assess similarity of air flow around geometrically similar objects of different scales.

- *Stk*: The *Stk* is a dimensionless ratio of the stopping distance of an aerosol particle to a characteristic dimension of the obstacle:

$$Stk = \frac{\rho_0 \mathrm{V} {d_a}^2 C_c}{d_c 18 \mu}$$

where d_a is the aerodynamic diameter of the particle, d_c is the characteristic dimension of the object (the probe diameter in our study), and C_c is the Cunningham slip correction factor, which can be ignored for particles larger than 1 μm.* It should also be noted that ρ_0 is standard density (1000 kg/m^3) and not particle density (ρ_p) or gas-fluid density(ρ_g), which is used in the previously described *Re* calculations.

When calculating *Stk* in an internal flow configuration, such as in a jet-impactor or a curved tube, the following equation is sometimes used:

$$Stk = \frac{\rho_0 \mathrm{V} {d_a}^2 C_c}{d_c 9 \mu}$$

where the "9" in the denominator comes from the use of the half-diameter of the jet or tube as the characteristic dimension. For example, this is done in the case of a jet impacting a plate

The *Stk* characterizes curvilinear motion of a particle in fluid flow and can also be thought of as the ratio of the time it takes a particle to adjust to streamline curvature to the time available for the adjustment.* Therefore, as *Stk* increases, the particles will deviate more from the flow streamlines. Notice that *Stk* is calculated using d^2. Hence, it is common practice to show data as a function of $\sqrt{Stk}$, so that it is directly proportional to particle size.

*Hinds, W. *Aerosol Technology*; 2nd ed.; John Wiley & Sons: New York, NY, 1999.

DISTRIBUTION LIST

The following individuals and organizations were provided with one Adobe portable document format (pdf) electronic version of this report:

U.S. Combat Capabilities Development
Command Chemical Biological Center
(DEVCOM CBC)
FCDD-CBR-TS
ATTN: Wise, Daniel G.

DEVCOM CBC
Technical Library
FCDD-CBR-L
ATTN: Foppiano, S.
Stein, J.

Defense Technical Information Center
ATTN: DTIC OA

U.S. ARMY COMBAT CAPABILITIES DEVELOPMENT COMMAND
CHEMICAL BIOLOGICAL CENTER